NeuroToxicology xxx (2017) xxx–xxx

Contents lists available at ScienceDirect

NeuroToxicology

Full Length Article

Association of exposure to manganese and iron with striatal and thalamic GABA and other neurometabolites — Neuroimaging results from the WELDOX II study

Swaantje Casjens[a,*], Urike Dydak[b,c], Shalmali Dharmadhikari[b,c], Anne Lotz[a], Martin Lehnert[a], Clara Quetscher[a], Christoph Stewig[a], Benjamin Glaubitz[d], Tobias Schmidt-Wilcke[d,e], David Edmondson[b,c], Chien-Lin Yeh[b,c], Tobias Weiss[a], Christoph van Thriel[f], Lennard Herrmann[g], Siegfried Muhlack[g], Dirk Woitalla[g], Michael Aschner[h], Thomas Brüning[a,1], Beate Pesch[a,1]

[a] Institute for Prevention and Occupational Medicine of the German Social Accident Insurance, Institute of the Ruhr-Universität Bochum (IPA), Bochum, Germany
[b] School of Health Sciences, Purdue University, West Lafayette, IN, USA
[c] Department of Radiology and Imaging Sciences, Indiana University School of Medicine, Indianapolis, IN, USA
[d] Department of Neurology, BG University Hospital Bergmannsheil, Ruhr-Universität Bochum, Bochum, Germany
[e] Institute of Clinical Neuroscience and Medical Psychology, University of Düsseldorf, Düsseldorf, Germany
[f] Leibniz Research Centre for Working Environment and Human Factors (IfADo), Dortmund, Germany
[g] Department of Neurology, Sankt Josef Hospital, Bochum, Germany
[h] Department of Molecular Pharmacology, Albert Einstein College of Medicine, New York, NY, USA

ARTICLE INFO

Article history:
Received 27 April 2017
Received in revised form 24 July 2017
Accepted 7 August 2017
Available online xxx

Keywords:
Welders
Globus pallidus
Magnetic resonance spectroscopy
Glutamate
Parkinson
Haemochromatosis

ABSTRACT

Objective: Magnetic resonance spectroscopy (MRS) is a non-invasive method to quantify neurometabolite concentrations in the brain. Within the framework of the WELDOX II study, we investigated the association of exposure to manganese (Mn) and iron (Fe) with γ-aminobutyric acid (GABA) and other neurometabolites in the striatum and thalamus of 154 men.

Material and methods: GABA-edited and short echo-time MRS at 3T was used to assess brain levels of GABA, glutamate, total creatine (tCr) and other neurometabolites. Volumes of interest (VOIs) were placed into the striatum and thalamus of both hemispheres of 47 active welders, 20 former welders, 36 men with Parkinson's disease (PD), 12 men with hemochromatosis (HC), and 39 male controls. Linear mixed models were used to estimate the influence of Mn and Fe exposure on neurometabolites while simultaneously adjusting for cerebrospinal fluid (CSF) content, age and other factors. Exposure to Mn and Fe was assessed by study group, blood concentrations, relaxation rates R1 and R2* in the globus pallidus (GP), and airborne exposure (active welders only).

Results: The median shift exposure to respirable Mn and Fe in active welders was 23 μg/m^3 and 110 μg/m^3, respectively. Airborne exposure was not associated with any other neurometabolite concentration. Mn in blood and serum ferritin were highest in active and former welders. GABA concentrations were not associated with any measure of exposure to Mn or Fe. In comparison to controls, tCr in these VOIs was lower in welders and patients with PD or HC. Serum concentrations of ferritin and Fe were associated with *N*-acetylaspartate, but in opposed directions. Higher R1 values in the GP correlated with lower neurometabolite concentrations, in particular tCr ($\exp(\beta) = 0.87$, $p < 0.01$) and choline ($\exp(\beta) = 0.84$, $p = 0.04$). R2* was positively associated with glutamate-glutamine and negatively with *myo*-inositol.

Conclusions: Our results do not provide evidence that striatal and thalamic GABA differ between Mn-exposed workers, PD or HC patients, and controls. This may be due to the low exposure levels of the Mn-exposed workers and the challenges to detect small changes in GABA. Whereas Mn in blood was not

* Corresponding author at: Institute for Prevention and Occupational Medicine of the German Social Accident Insurance, Institute of the Ruhr–Universität Bochum (IPA), Bürkle–de–la–Camp–Platz 1, 44789 Bochum, Germany.
E-mail address: casjens@ipa-dguv.de (S. Casjens).
[1] Authors contributed equally.

http://dx.doi.org/10.1016/j.neuro.2017.08.004

associated with any neurometabolite content in these VOIs, a higher metal accumulation in the GP assessed with R1 correlated with generally lower neurometabolite concentrations.

1. Introduction

Manganese (Mn) is an essential trace element naturally found in the environment. It is required for a variety of key physiological processes (Chen et al., 2015). Commonly, sufficient amounts of Mn are supplied by the diet; however, occupational settings, such as Mn mining (Myers et al., 2003), steel and alloy production (Bouchard et al., 2008) or welding (Ellingsen et al., 2014; Long et al., 2014a; Pesch et al., 2012) present increased risks for systemic exposure and brain accumulation of this metal (Fitsanakis et al., 2006). In addition to Mn, iron (Fe) is a major constituent of welding fume (Flynn and Susi, 2010; Pesch et al., 2012). Both metals share biological transport systems due to their structural similarity, partly indicated by a negative association of Mn in blood (MnB) and serum ferritin (SF) (Aguirre and Culotta, 2012). Mn accumulates in brain regions susceptible to oxidative stress, preferentially in the globus pallidus (GP) (Bowman and Aschner, 2014). Fe accumulates preferentially in the substantia nigra (SN), where Fe, dopamine and neuromelanin are linked to the etiology brain aging and Parkinson's disease (PD) (Jiang et al., 2016; Zucca et al., 2015). Several studies visualized Mn and Fe accumulation in the brain by using increased T1-weighted/R1 and T2*-weighted/R2* signals in magnetic resonance imaging (MRI) (Lee et al., 2015, 2016; Long et al., 2014a).

Various neurological dysfunctions have been recognized ranging from subclinical neurobehavioral effects associated with low Mn exposure to manganism as a neurodegenerative disease following high exposure (Iannilli et al., 2016; Mergler et al., 1999; Racette et al., 2017; Zoni and Lucchini, 2013). Brain metabolites have been proposed as markers for an early detection of Mn neurotoxicity before structural damage can be ascertained (Zheng et al., 2011). Furthermore, changes in brain Fe status have been shown to modify neurometabolite homeostasis (Kim and Wessling-Resnick, 2014). Within the framework of the WELDOX II study, magnetic resonance spectroscopy (MRS) was used to quantify neurometabolites for an investigation of the effects of airborne or systemic Mn and Fe on brain metabolism in the striatum and thalamus. MRS allows estimating the content of neurometabolites such as γ-aminobutyric acid (GABA; major inhibitory neurotransmitter), total creatine (tCr; involved in energy metabolism), *N*-acetylaspartate (NAA; a marker of general neuronal function), *N*-acetylaspartylglutamate (NAAG; most concentrated peptide in the brain), *myo*-inositol (mI; a glial cell marker), glutamate (Glu; an excitatory neurotransmitter), glutamine (Gln; precursor of Glu and GABA), and choline-containing compounds (Cho; an indicator of cell membrane integrity) in the selected brain regions (Dydak et al., 2011).

Several MRS studies have linked occupational exposure to Mn and Fe or PD to changes in neurometabolite concentrations (Dydak et al., 2016; Guilarte, 2013). Thalamic GABA was elevated in smelters (Dydak et al., 2011; Long et al., 2014b) and PD patients (Dharmadhikari et al., 2015). However, results on striatal GABA concentrations in PD are controversial (Dharmadhikari et al., 2015; Emir et al., 2012). Furthermore, thalamic mI was reduced in welders and smelters (Long et al., 2014a). Other neurometabolites (Cho and Glu) were not altered in various brain regions (Chang et al., 2009; Dydak et al., 2011; Kim et al., 2007). Non-human primates exposed to Mn showed a significant decrease of NAA/Cr in the parietal cortex, but not in striatum, thalamus and frontal white matter, and no alterations were reported for other metabolites (Cho, mI) (Guilarte et al., 2006). In rodents, the main neurochemical effect was an increase in striatal GABA concentrations throughout a wide range of Mn exposures (Gwiazda et al., 2007).

The aim of this analysis within the framework of the WELDOX II study was to explore the association of diverse measures of exposure to Mn and Fe with the content of neurometabolites in volumes of interests (VOIs) placed in thalamus and striatum of both hemispheres. Considering prior reports on alterations in the GABAergic system, the hypokinetic nature of parkinsonism symptoms and the excitatory projection of the thalamus to cortical regions in the motor pathway, we hypothesized welders will show increased thalamic concentration of the inhibitory neurotransmitter GABA. Due to the importance of Glu in basal ganglia pathways and the fact that Glx is co-edited in GABA-edited spectra, and the reported changes in NAA and mI in Mn exposure (Chang et al., 2009; Dydak et al., 2011; Guilarte et al., 2006; Kim et al., 2007), as well as the reported changes in tCr, Cho and mI in PD and neurodegenerative diseases in general (Dydak et al., 2016; Öz et al., 2014), all these neurochemicals were included in our models. Metal exposure was assessed with a comparison of study groups being at-risk occupations (active and former welders), patients with PD or hemochromatosis (HC), and controls recruited from the general population. Furthermore, biomarkers in the blood and brain as well as airborne exposure in active welders were analyzed. To our knowledge, this is the first study to investigate the effect of both redox-active metals on the concentrations of GABA, NAA and other neurometabolites in the living human brain in such an extensive manner.

2. Material and methods

2.1. Study population

In total, 174 participants were recruited for the neuroimaging study WELDOX II from 2013 to 2016. Eligible men were 45 years or older and did not meet any exclusion criterion (claustrophobia, metal fragments in the eyes, carrying a cardiac pacemaker or cochlear implant, large tattoos). For this analysis, participants were excluded if MRS data was completely missing, brain neoplasms or other pathologic changes were detected during MRI, Fe status and MnB were incomplete, or GABAergic medication was taken. Here, the study population comprised 154 men: 47 active welders, 20 former welders, 39 controls, 36 PD patients, and 12 HC patients).

Active welders were recruited from 14 companies located in different areas of North Rhine-Westphalia.Twenty-one welders (45%) performed gas metal arc welding (GMAW) with solid or flux-cored wire. Most of the other welders performed tungsten inert gas welding (TIG). Personal exposure to respirable welding fume was measured in the breathing zone during a working shift. Post-shift blood samples were drawn for the determination of Mn. Neuroimaging and neurological examination of active welders was conducted about six weeks later in the study center.

Former welders and controls were recruited from the general population of the greater Bochum area. Controls were eligible if they had never worked as welder and did not suffer from diseases that may impair motor function. PD patients were enrolled from the department of neurology of the Sankt Joseph Hospital in Bochum. HC patients were recruited through their self-help organization.

Please cite this article in press as: S. Casjens, et al., Association of exposure to manganese and iron with striatal and thalamic GABA and other neurometabolites — Neuroimaging results from the WELDOX II study, Neurotoxicology (2017), http://dx.doi.org/10.1016/j.neuro.2017.08.004

All participants provided a blood sample for the determination of the blood count and laboratory diagnostics of Fe metabolism, including SF and serum Fe (SFe), gamma-glutamyl transferase (GGT) and other liver enzymes at the day of neuroimaging at the Institute of Clinical Chemistry, Transfusion and Laboratory Medicine of the Berufsgenossenschaftliches University Hospital Bergmannsheil with methods as formerly described for the WELDOX study (Casjens et al., 2014). GGT $\geq$ 56 U/L (90th percentile) was considered as indicative for a potential liver dysfunction. In addition, carbohydrate-deficient transferrin (CDT) was determined and values $>$ 2.6% were used to indicate a risk for alcohol abuse.

Socio-demographic characteristics, occupational history, medications, and chronic diseases were assessed by questionnaire. A supplemental questionnaire for welders documented their welding history. All participants underwent a neurological assessment of movement disorders by a neurologist (MDS UPDRS rating) and further examinations, e.g. fine motor test, odor identification, and balance tests.

All participants provided written informed consent. The study protocol was approved by the Ethics Committee of the Ruhr University Bochum, Germany.

2.2. Airborne exposure to Mn and Fe

Personal air sampling was performed in all active welders. The concentrations of respirable Mn and Fe were measured as previously described (Pesch et al., 2012). PGP-EA samplers were used for collecting respirable particles at a flow rate of 3.5 L/min in the breathing zone of the active welders (Lehnert et al., 2012). Sampling duration was four hours on average. Mn and Fe were determined by inductively coupled plasma mass spectrometry (ICP-MS) with a Perkin Elmer Elan DRC II (Waltham, Massachusetts). The samples were prepared according to a standard protocol (Hebisch et al., 2005). For the statistical analyses, measurements below the limits of quantitation (LOQs) were converted to 0.5 * LOQ (Mn: one measurement <LOQ, Fe: four measurements < LOQ). The German occupational exposure limit (OEL) for respirable Mn is 20 $\mu g/m^3$ (https://www.baua.de/DE/Angebote/Rechtstexte-und-Technische-Regeln/Regelwerk/TRGS/TRGS-900.html). No German OEL has been established for respirable Fe.

2.3. Determination of Mn in whole blood

MnB was determined at the Institute for Prevention and Occupational Medicine of the German Social Accident Insurance by means of inductively coupled plasma-quadrupole mass spectrometry (ICP-MS). Plastic materials were used for sample preparation to prevent metal contamination. Thawed blood samples (400 μL) were diluted 1:12.5 with a 0.5% solution of ammonium hydroxide and 100 μL of a 0.2% solution of Triton-X. Rhodium was used as internal standard. Analysis was carried out using a 7700 ICP-MS system from Agilent Technologies in He-mode (flow rate: 5 mL/min) with a collision cell to avoid interferences. Calibration and calculation of the Mn concentration were carried out using standards prepared in sheep blood at eight different concentrations. Materials from RECIPE (ClinChek Whole Blood Level, lyophil. for Trace Elements I and II, REF 8840, LOT 227) and SERONORM (Trace Elements Whole Blood Level I and II, LOT 1103129) served as internal control.

2.4. MRI and MRS data acquisition and processing

MRI scans were performed on a 3 T Philips Achieva X-series whole-body clinical scanner (Philips Healthcare, Best, The Netherlands) with a 32-channel head coil. R1 (1/T1) and R2* (1/T2*) relaxation rates were measured bilaterally in regions of interest (ROIs) placed in the GP, SN, and frontal lobe (FL). We performed the positioning in duplicate and used the arithmetic means of R1 respectively of R2* from both readers for the statistical analysis. T1-weighted 3D turbo field echo images (T1 TFE, TR/TE = 8.4/3.9 ms, flip angles = 8°, bandwidth = 191 Hz/pixel, 220 slices, voxel size 1 mm^3 isotropic, acquisition matrix: 240 $\times$ 240 mm, SENSE factor 2.5) were acquired for anatomical reference. Two fast field echo images (T1 FFE, TR/TE = 8.4/3.7 ms, flip angles = 3° and 17°, band width = 191 Hz/pixel, 160 slices, voxel size 1 mm^3 isotropic, acquisition matrix: 256 $\times$ 256 mm, SENSE factor 2) were used to estimate R1 in the ROIs. T1 values were calculated by the variable flip angle method (Sabati and Maudsley, 2013). T1 maps were corrected for field inhomogeneity by dual-TR B1 maps. Five 3D fast field echo images with different echo times (FFE, TR/TE/delta_TE = 24.3/3.7/4.4 ms, flip angle = 20°, bandwidth = 287 Hz/pixel, 80 slices, voxel size $(1.5\ mm)^3$ isotropic, acquisition matrix: 256 $\times$ 256 mm, SENSE factor 2) were acquired to estimate R2* in the ROIs. T2* values were calculated by fitting the signal intensity as a function of echo time using the exponential decay model (Long et al., 2014a).

Additionally, fast T2-weighted images (TR/TE = 6000/127 ms) in all three planes were acquired for planning the 30 mm $\times$ 30 mm $\times$ 25 mm MRS VOIs centered on the thalamus and on the striatum (head of caudate nucleus, putamen and part of GP interna) of both hemispheres. Brain tissue segmentation into gray matter (GM), white matter (WM), and cerebrospinal fluid (CSF) was based on superimposing the spectroscopy VOI coordinates on high resolution T1-weighted image using the partial volume correction tool by Nia Goulden and Paul Mullins (https://www.bangor.ac.uk/psychology/biu/Wiki.php.en) with the SPM Tool Segmentation (SPM8) as formerly described (Ashburner and Friston, 2005).

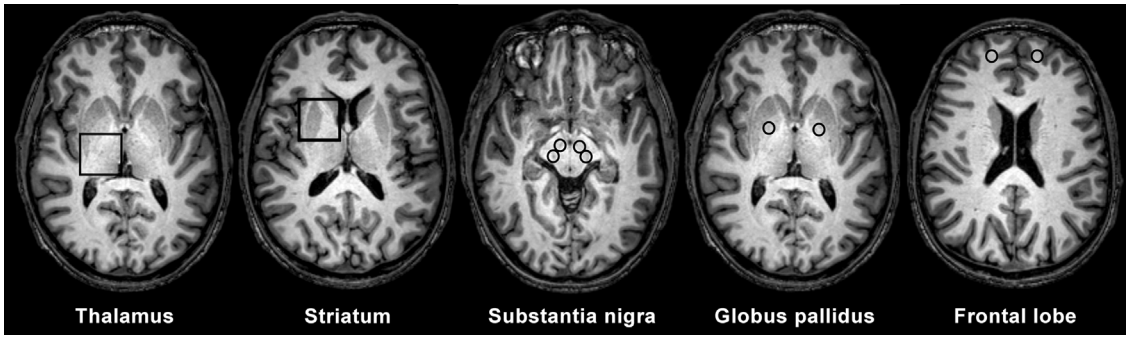

Fig. 1. Representative T1-weighted MRI brain images of an active welder with MRS voxels in the thalamus and striatum, and ROIs in the substantia nigra, globus pallidus and frontal lobe.

Please cite this article in press as: S. Casjens, et al., Association of exposure to manganese and iron with striatal and thalamic GABA and other neurometabolites — Neuroimaging results from the WELDOX II study, Neurotoxicology (2017), http://dx.doi.org/10.1016/j.neuro.2017.08.004

Both, short echo time point resolved spectroscopy (PRESS) spectra (echo time (TE) = 30 ms, repetition time (TR) = 2000 ms, 32 averages) and MEGA-PRESS edited GABA spectra (TE/TR = 68/2000 ms, edit ON acquisitions = 16, edit OFF acquisitions = 16) were acquired from each VOI. In conventional MRS the GABA peak is overlaid by the much larger tCr peak. Therefore, the special GABA-editing MRS technique MEGA-PRESS is used, allowing for a better detection of the small GABA signal (Mullins et al., 2014). In addition, reference spectra without water suppression were obtained for phase, frequency and eddy current correction.

Post-processing and quantification of GABA spectra were done in LCModel (v 6.2-0R), a spectral quantification tool that fits each spectrum as a weighted linear combination of basis spectra from individual brain metabolites (Provencher, 1993). The basis set included Glu, Gln, tCr, glycerophosphocholine (GPC), phosphocholine (PCh), NAA, NAAG, mI, and several minor metabolites. Furthermore, three metabolite sums were examined: Glx = Glu + Gln, total choline (Cho) = GPC + Ph, and total NAA = NAA + NAAG. All neurometabolite concentrations were scaled with respect to the unsuppressed water signal. Tissue correction of neurometabolite content is commonly applied to correct the acquired MRS data for the segmentation of VOIs, assuming no metabolic activity in CSF. For descriptive analyses CSF-corrected concentrations [mM] were presented (Chowdhury et al., 2015). However, for the regression models water-scaled metabolite values in institutional units [i.u.] were used and CSF content was included in the regression models together with other covariates such as age or smoking in addition to exposure measures.

LCModel also provides an estimated relative standard deviation (%SD) for each metabolite as a measure of the believability of the concentration values reported. Only results with%SD values $< 20\%$ were used for further statistical analysis.

An example of the MRS VOIs and MRI ROIs is shown in Fig. 1.

2.5. Statistics

All calculations were done using SAS, version 9.4 (SAS Institute Inc., Cary, NC, USA). Continuous variables were described with median and inter-quartile range (IQR). For descriptive purposes, we presented the arithmetic mean from the left and right hemisphere of GABA and each other neurometabolite. The distribution of the exposure variables in welders were stratified by welding technique (GMAW *vs.* other technique). Rank correlations between variables were presented by Spearman's correlation coefficient (r_S) with 95% confidence interval (CI). In addition, partial Spearman correlation coefficients (r_{sp}) with 95% CIs were used to describe the associations between neurometabolites, while controlling for CSF content in the VOIs. Linear mixed models were applied to the log-transformed striatal and thalamic neurometoblite concentrations to estimate the influence of exposure to Mn and Fe while controlling for other covariates. The study group and the exposure variables were fixed factors. We chose subject as random factor to consider the dependence of the four measurements in both brain regions (striatum, thalamus) and hemisphere (left, right) per subject. Additionally, linear mixed models were applied in active welders to investigate the association of neurometabolites with airborne Mn and Fe. All models were adjusted for age, smoking status (never, former, current), CDT ($\leq 2.6\%$, $> 2.6\%$), and CSF content [%].

Table 1
Socio-demographic characteristics, manganese in blood, and iron status of the WELDOX II study population.

	Total		Active welders		Former welders		Parkinson patients		Haemochromatosis patients		Controls	
n	154		47		20		36		12		39	
Age [years] (median, IQR)	56	50; 64	50	47; 55	65	56.5; 69	60	55; 67	56	51.5; 67	54	50; 64
Education (n, %)												
Lower secondary school or no qualification	74	48.1%	31	66.0%	16	80.0%	17	47.2%	2	16.7%	8	20.5%
Intermediate school	33	21.4%	14	29.8%	3	15.0%	7	19.4%	1	8.3%	8	20.5%
University entrance level	47	30.5%	2	4.3%	1	5.0%	12	33.3%	9	75.0%	23	59.0%
Longest occupation as blue-collar worker (n, %)	105	68.2%	47	100%	20	100%	19	52.8%	3	25.0%	16	41.0%
Smoking status (n, %)												
Never	50	32.5%	10	21.3%	1	5.0%	16	44.4%	7	58.3%	16	41.0%
Former	57	37.0%	14	29.8%	11	55.0%	14	38.9%	5	41.7%	13	33.3%
Current	47	30.5%	23	48.9%	8	40.0%	6	16.7%	0	0%	10	25.6%
Carbohydrate-deficient transferrin [%]												
Median, inter-quartile range	1.0	0.8; 1.2	1.1	0.9; 1.4	1.0	0.8; 1.4	0.9	0.8; 1.1	0.8	0.7; 0.9	0.9	0.8; 1.1
>2.6 (n, %)	8	5.2%	4	8.5%	2	10.0%	0	0%	0	0%	2	5.1%
Gamma-glutamyl transferase [U/L]												
Median, inter-quartile range	34	22; 53	35	22; 54	47.5	34; 69.5	31	21.5; 46	24.5	15; 33.5	29	22; 50
≥ 56 (n, %)	28	18.2%	9	19.1%	7	35.0%	6	16.7%	0	0%	6	15.4%
Manganese in blood [μg/L] (median, IQR)	6.8	5.8; 8.4	7.6	6.7; 9.3	6.4	5.6; 8.3	6.3	5.2; 7.7	6.2	5.6; 8.5	6.5	5.9; 7.2
Serum ferritin [μg/L] (median, IQR)	111.5	64; 188	131	80; 233	241.5	111; 434	108.5	70.5; 189	44	29.5; 186	74	55; 112
Serum iron [μg/dL] (median, IQR)	103	84; 121	103	85; 120	93.5	65.5; 134	95	79; 115	121.5	104; 169	105	92; 122
R1, globus pallidus [1/ms] (median, IQR)	0.85	0.81; 0.91	0.88	0.84; 0.93	0.82	0.78; 0.85	0.85	0.82; 0.92	0.85	0.80; 0.89	0.82	0.79; 0.87
R1, substantia nigra [1/ms] (median, IQR)	0.76	0.71; 0.80	0.75	0.72; 0.8	0.79	0.72; 0.83	0.76	0.72; 0.8	0.78	0.7; 0.82	0.73	0.67; 0.76
R1, frontal lobe [1/ms] (median, IQR)	0.95	0.90; 1.00	0.96	0.93; 1.03	0.90	0.88; 0.96	0.97	0.91; 1.01	0.96	0.90; 0.98	0.93	0.86; 0.98
R2*, globus pallidus [1/ms] (median, IQR)	41.2	37.8; 46.2	40.1	36.8; 46.5	41.4	38.2; 44.4	43.0	40.1; 47.7	44.2	37.9; 47.2	37.7	35.9; 44.0
R2*, substantia nigra [1/ms] (median, IQR)	44.8	39.5; 51.7	41.8	38.9; 46.9	44.9	40.9; 55.9	45.3	40.4; 50.8	48.4	39.6; 60.0	42.3	37.8; 49.8
R2*, frontal lobe [1/ms] (median, IQR)	22.0	20.9; 23.2	21.7	20.3; 22.8	22.0	21.6; 23.3	22.4	20.9; 23.9	22.0	21.2; 23.0	21.1	20.7; 22.3
Respirable manganese [$\mu g/m^3$]			23	4.7; 86								
Respirable iron [$\mu g/m^3$]			110	14; 400								

IQR: inter-quartile range; R1 and R2*: arithmetic mean of both hemispheres.

Please cite this article in press as: S. Casjens, et al., Association of exposure to manganese and iron with striatal and thalamic GABA and other neurometabolites — Neuroimaging results from the WELDOX II study, Neurotoxicology (2017), http://dx.doi.org/10.1016/j.neuro.2017.08.004

3. Results

3.1. Demographics and covariates of the exposure to Mn and Fe

Table 1 depicts the distribution of socio-demographic characteristics and biomarkers of exposure to Mn and Fe (blood: MnB, SF, SFe; brain: R1, R2* in ROIs) in 154 participants of WELDOX II. The median age of all men was 56 years (IQR 50–64). Active and former welders worked long-term in this occupational setting (median 27 years (IQR 24–33) and 33 years (IQR 27–43), respectively). On average, former welders were not exposed to welding fumes for seven years. The fractions of blue-collar jobs as longest held occupation were 100% in all welders, 41% in controls, 53% in PD, and 25% in HC. More welders smoked at some point in their lives and had a lower education than the other study groups. GGT above the reference value of 56 U/L was observed in 19% of active and in 35% of the former welders, in 15% of controls and in 17% of patients with PD, but in none of the HC patients. Six out of eight men with CDT >2.6% were welders, but we observed none of the patients with PD or HC with elevated CDT.

Median MnB ranged from 7.6 μg/L (IQR 6.7–9.3) in active welders to 6.2 μg/L (IQR 5.6–8.5) in HC patients. Median SF was highest in former welders (241.5 μg/L, IQR 111–434) and lowest in HC (44 μg/L, 29.5–186). A similar pattern was shown for transferrin. On the other hand, we observed an opposite pattern for SFe (former welders: 93.5 μg/dL, PD: 95 μg/dL, HC: 121.5 μg/dL). Active welders had similar median concentrations of SFe as controls (103 μg/dL and 105 μg/dL), but a higher median of SF (131 μg/L and 74 μg/L, respectively). The medians of R1 in GP ROIs reflect partially the ranking of MnB being highest in active welders and lowest in HC. The medians of the corresponding R2* values were also lowest in HC but highest in PD.

The median exposure to respirable Mn and Fe in active welders was 23 $\mu g/m^3$ (IQR 4.7-86) and 110 $\mu g/m^3$ (IQR 14–400), respectively. GMAW was used by 21 active (45%) and 13 former welders (65%). Median shift exposure to respirable Mn and Fe were higher when using GMAW (Mn: 57 (IQR 33–130) $\mu g/m^3$, Fe: 360 (IQR 190–750) $\mu g/m^3$) than TIG and other techniques (Mn: 5 (IQR 2–23) $\mu g/m^3$, Fe: 15 (IQR 5–84) $\mu g/m^3$). In active, but not in former welders, MnB and SF were higher when using GMAW. The neurometabolite concentrations did not differ between welding techniques. For more details see Supplemental Table S1.

3.2. Distribution of neurometabolites in the striatum and thalamus

We measured neurometabolites in both hemispheres. Concentrations in the right and left hemispheres were correlated, especially in the thalamus (data not shown). However, striatal GABA, Glu and Glx did not correlate between the two hemispheres.

Table 2 depicts the distribution of different brain tissue contributions in the voxels and the content of neurometabolites as arithmetic mean of both hemispheres in the VOIs placed in striatum and thalamus. As expected, the tissue content of the striatum voxels differed from that in the thalamus (e.g. GM_{Str} 32.5% *vs.* GM_{Thal} 20.9%, WM_{Str} 55% *vs.* WM_{Thal} 70.7%) with minor differences between the study groups. In general, the CSF content was low (CSF_{Str} 12.0%, CSF_{Thal} 8.3%). As shown in Supplemental Table S2, the neurometabolite concentrations correlated negatively with the CSF content of the VOIs and frequently positively with the GM and WM content.

The GABA concentration was 2.0 mM in the striatal and thalamic VOIs and did not differ between the study groups. The concentrations of other neurometabolites varied slightly between brain regions and groups as shown in Table 2. Glx and tCr were higher in the striatum but NAA was lower as compared with the VOIs in the thalamus. Striatal tCr was highest in controls. Supplemental Table S2 also shows significant correlations of the respective neurometabolites measured in striatum *vs.* thalamus adjusted for the CSF content. Thalamic GABA was not correlated with other neurometabolites in this brain region

Table 2
Median and inter-quartile ranges (IQR) of striatal and thalamic tissue content and neurometabolite concentrations in the study groups of WELDOX II.

	Total		Welders		Former welders		Controls		Parkinson patients		Haemochromatosis patients	
	Median	IQR	Median	IQR	Median	IQR	Median	IQR	Median	IQR	Median	IQR
Striatum												
Grey matter [%]	32.5	30.3; 35.1	32.1	29.5; 35.5	32.6	31.0; 35.3	33.6	31.0; 36.6	31.6	29.9; 33.6	31.7	29.7; 33.7
White matter [%]	55.0	52.1; 57.7	55.4	52.4; 57.5	54.7	51.8; 56	55.2	52.7; 57.3	54.3	50.8; 58.4	54.4	53.0; 58.0
Cerebrospinal fluid [%]	12.0	9.0; 15.1	11.2	9.0; 15.7	12.4	8.7; 14.5	11.1	7.9; 13.2	13.2	9.9; 16.7	13.1	10.1; 15.7
γ-aminobutyric acid (GABA) [mM]	2.0	1.8; 2.2	2.0	1.8; 2.2	1.9	1.7; 2.1	1.9	1.8; 2.0	2.0	1.8; 2.2	2.1	1.8; 2.5
Glutamate [mM]	6.7	5.9; 7.3	6.8	6.2; 7.3	6.6	5.9; 6.9	6.8	5.8; 7.3	6.7	5.9; 7.5	6.1	5.4; 6.3
Glutamate and glutamine [mM]	10.3	9.1; 11.3	10.2	9.1; 11.4	10.0	9.1; 11.0	10.5	9.3; 11.3	10.5	9.1; 11.7	9.9	9.0; 10.6
Total creatine [mM]	7.1	6.7; 7.6	7.1	6.7; 7.5	6.9	6.7; 7.3	7.4	6.9; 7.8	7.2	6.5; 7.6	6.9	6.3; 7.2
Total choline [mM]	2.2	2.0; 2.4	2.2	1.9; 2.4	2.0	1.9; 2.3	2.3	2.0; 2.5	2.2	2.1; 2.6	2.1	2.0; 2.4
N-acetyl aspartate (NAA) [mM]	6.4	5.9; 6.8	6.5	6.1; 6.8	6.1	5.5; 6.9	6.6	6.1; 6.9	6.4	5.8; 6.9	6.4	5.5; 6.5
Total NAA [mM]	6.6	6.2; 7.1	6.7	6.2; 7.2	6.4	5.9; 7.1	6.6	6.3; 6.9	6.6	6.1; 7.1	6.5	6.1; 6.8
Myo-inositol [mM]	4.4	3.9; 4.8	4.4	4.0; 4.7	4.1	3.8; 5.0	4.3	3.9; 4.7	4.4	3.9; 5.0	4.4	4.0; 4.6
Thalamus												
Grey matter [%]	20.9	19.5; 22.3	21.0	19.2; 22.1	21.6	19.8; 23.2	20.7	19.2; 22.3	20.9	19.7; 21.8	21.3	20.0; 23.8
White matter [%]	70.7	67.4; 73.5	70.1	66.9; 73.5	69.7	66.6; 70.9	73.2	69.8; 75.1	70.7	67.1; 73.0	69.4	67.9; 71.2
Cerebrospinal fluid [%]	8.3	5.7; 10.7	8.7	6.4; 10.8	10.1	7.5; 11.0	5.7	4.6; 8.5	8.6	6.4; 10.9	9.3	6.8; 10.8
GABA [mM]	2.0	1.8; 2.3	2.0	1.7; 2.2	2.0	1.8; 2.3	1.9	1.7; 2.4	2.1	1.9; 2.4	1.9	1.6; 2.1
Glutamate [mM]	5.5	5.0; 6.1	5.9	5.4; 6.3	5.6	5.0; 6.2	5.3	5.0; 5.9	5.5	5.0; 5.9	5.3	4.6; 6.0
Glutamate and glutamine [mM]	7.8	6.8; 8.9	8.0	7.3; 9.1	8.4	6.3; 9.2	7.0	6.4; 8.3	7.6	6.8; 8.5	7.5	6.6; 9.6
Total creatine [mM]	6.4	6.1; 6.8	6.6	6.2; 6.8	6.4	6.1; 6.7	6.3	6.1; 6.7	6.3	6.0; 6.8	6.1	6.1; 6.7
Total choline [mM]	2.1	2.0; 2.2	2.1	2.0; 2.3	2.0	1.9; 2.3	2.0	1.9; 2.1	2.1	2.0; 2.2	2.1	1.9; 2.2
NAA [mM]	6.8	6.4; 7.2	7.0	6.5; 7.3	6.8	6.4; 7.1	6.7	6.2; 7.2	6.9	6.3; 7.3	6.8	6.6; 7.3
Total NAA [mM]	7.5	7.0; 8.0	7.9	7.3; 8.3	7.5	6.9; 7.9	7.4	7.0; 7.8	7.4	6.8; 7.9	7.5	7.1; 7.8
Myo-inositol [mM]	4.7	4.2; 5.1	4.7	4.1; 5.1	4.6	4.1; 5.1	4.6	4.2; 4.8	4.8	4.2; 5.4	4.5	4.1; 5.0

Neurometabolites: arithmetic mean of both hemispheres.

Please cite this article in press as: S. Casjens, et al., Association of exposure to manganese and iron with striatal and thalamic GABA and other neurometabolites — Neuroimaging results from the WELDOX II study, Neurotoxicology (2017), http://dx.doi.org/10.1016/j.neuro.2017.08.004

whereas Glx, NAA and tCr showed significant associations (Glx and tCr $r_{Sp} = 0.32$). By contrast, striatal GABA was correlated with Glx and tCr and showed marginal positive associations with the other metabolites.

Supplemental Table S3 presents the correlations of neurometabolites adjusted for the CSF content with age, biomarkers for Mn and Fe in blood and brain in all participants and for airborne Mn and Fe in active welders only. We observed no clear pattern of the associations between the other neurometabolites and exposure to Mn or Fe in air, blood or assessed with the surrogate markers R1 and R2* for metal accumulation in the GP. The associations observed in the striatum were mostly weaker than in the thalamus. These correlations were not adjusted for covariates or multiple tests. We account for the complex influences of neuroanatomy, age and exposure in the statistical models presented in Table 3.

3.3. Potential predictors of neurometabolites

The effect estimates for the various exposure measures and potential confounders of the neurometabolites assessed with mixed linear regression models using MRS measurements of both assessed brain regions and hemispheres of the participants are shown in Table 3. The level-two variance estimates reflect the correlations between the neurometabolite concentrations of the four VOIs.

In all models, we adjusted the potential influence of exposure to Mn or Fe for smoking, CDT, age, and%CSF. In addition, we included the results in both brain regions and hemispheres. As expected, a higher CSF content and higher attained age resulted in decreased neurometabolite concentrations. Concentrations of GABA, NAA, total NAA, and mI were lower in the striatum than in the thalamus and *vice versa* for Glu, Glx, and tCr. Smoking status played a subordinate role with smokers having lower GABA concentrations than never smokers, and former smokers having higher concentrations in all other neurometabolites than never smokers. CDT > 2.6% was associated with lower concentrations of most neurometabolites, especially in total NAA with $\exp(\beta) = 0.95$ ($p = 0.04$).

We successively implemented the five different exposure variables in the various models. We observed no influence of any exposure measure on GABA. In model 1, being a welder or a patient with PD or HC was compared to controls. tCr was lower in these study groups than in controls. The effects of systemic exposure (MnB and iron status) on neurometabolite concentrations are investigated in model 2. Whereas MnB was only marginally associated with total NAA ($p = 0.07$), SF and SFe influenced NAA and total NAA in opposite directions. In model 3, higher R1 values resulted in lower neurometabolite concentrations with significant outcomes for tCr ($\exp(\beta) = 0.87$, $p = 0.005$) and Cho ($\exp(\beta) = 0.84$, $p = 0.04$) and marginally for Glu and NAA. Higher R2* values resulted in higher concentrations of Glx and lower concentrations of mI. R1 and R2* in the SN and FL did not affect neurometabolite concentrations (data not shown). Respirable Mn and Fe did not influence the neurometabolite content among active welders (models 4 and 5).

Table 3
Potential predictors of neurometabolites estimated with separate mixed linear regression models for five different exposure settings.Statistically significant results are marked in bold.

	GABA [i.u.]		Glu [i.u.]		Glx [i.u.]		tCr [i.u.]		Cho [i.u.]		NAA [i.u.]		Total NAA [i.u.]		mI [i.u.]	
	exp (β)	P value	exp (β)	P value	exp (β)	P value	exp (β)	P value	exp (β)	P value	exp (β)	P value	exp (β)	P value	exp (β)	P value
Model 1																
Intercept	1.746		5.580		8.452		6.405		1.965		6.786		7.357		3.845	
Active welders *vs.* controls	1.017	0.60	1.039	0.13	1.030	0.34	**0.967**	**0.02**	0.993	0.78	1.005	0.80	1.028	0.09	1.003	0.92
Former welders *vs.* controls	1.020	0.64	1.011	0.74	1.023	0.59	0.976	0.19	0.970	0.32	0.989	0.65	1.008	0.71	0.968	0.37
Parkinson patients *vs.* controls	1.020	0.53	0.996	0.88	1.021	0.51	**0.969**	**0.03**	1.023	0.36	0.983	0.38	0.986	0.39	1.017	0.55
Haemochromatosis patients *vs.* controls	1.025	0.62	0.936	0.09	0.989	0.83	**0.940**	**0.005**	0.969	0.38	0.963	0.18	0.975	0.31	0.994	0.88
Former *vs.* never smokers	0.984	0.56	1.034	0.13	**1.057**	**0.04**	1.019	0.14	1.031	0.15	1.005	0.74	1.020	0.17	**1.062**	**0.02**
Current *vs.* never smokers	0.967	0.27	0.977	0.33	0.988	0.69	1.000	1.00	0.993	0.74	0.972	0.11	0.978	0.15	1.004	0.88
CDT > 2.6% *vs.* ≤ 2.6%	0.990	0.84	0.958	0.29	0.914	0.08	0.971	0.20	0.957	0.26	**0.942**	**0.05**	**0.948**	**0.04**	1.063	0.19
Age [per 10 years]	1.012	0.47	0.980	0.11	**0.957**	**0.007**	0.987	0.06	0.990	0.42	0.989	0.24	0.990	0.21	1.009	0.51
Cerebrospinal fluid [%]	**0.989**	**< 0.001**	**0.993**	**< 0.001**	0.996	0.10	**0.993**	**< 0.001**	**0.996**	**0.01**	**0.990**	**< 0.001**	**0.990**	**< 0.001**	**0.993**	**< 0.001**
Striatum *vs.* thalamus	**0.958**	**0.03**	**1.146**	**< 0.001**	**1.261**	**< 0.001**	**1.080**	**< 0.001**	1.011	0.35	**0.909**	**< 0.001**	**0.856**	**< 0.001**	**0.914**	**< 0.001**
Model 2[a]																
Mn in blood [log μg/L]	0.964	0.34	1.054	0.11	1.031	0.45	1.009	0.65	0.998	0.95	1.033	0.16	1.039	0.07	0.953	0.19
Serum ferritin [log μg/L]	1.005	0.68	1.001	0.91	0.996	0.78	0.992	0.18	1.001	0.95	**0.980**	**0.005**	0.991	0.17	1.010	0.39
Serum iron [log μg/dL]	1.015	0.61	1.009	0.70	1.045	0.14	1.000	0.98	0.997	0.90	**1.045**	**0.009**	**1.035**	**0.02**	0.994	0.83
Model 3[a]																
R1, globus pallidus [log 1/ms]	0.829	0.11	0.850	0.08	0.845	0.14	**0.867**	**0.005**	**0.835**	**0.04**	0.887	0.07	0.920	0.16	0.957	0.66
R2*, globus pallidus [log 1/ms]	0.919	0.16	1.083	0.11	**1.137**	**0.04**	1.020	0.46	1.027	0.55	0.989	0.75	0.975	0.41	**0.892**	**0.03**
Model 4[a]																
Respirable Mn [log μg/m^3]	1.006	0.63	1.002	0.84	0.998	0.86	1.002	0.61	1.001	0.89	0.995	0.45	0.998	0.79	1.007	0.56
Model 5[a]																
Respirable iron [log μg/m^3]	1.006	0.52	0.997	0.68	0.990	0.35	1.000	0.98	0.997	0.65	0.993	0.17	0.995	0.25	1.008	0.36

Model 1: At-risk occupation or disease; Model 2: Systemic exposure; Model 3: Brain exposure; Model 4: Airborne exposure to Mn in active welders; Model 5: Airborne exposure to iron in active welders; GABA: γ-aminobutyric acid; Glu: glutamate; Glx: Glu and glutamine; tCr: total creatine; Cho: choline-containing compounds; NAA: N-acetylaspartate; mI: *myo*-inositol; Mn: manganese; CDT: Carbohydrate-deficient transferrin; [a]These models are adjusted by age [10 years], smoking status (never, former, current), CDT (≤2.6%, >2.6%), brain region (striatum, thalamus), cerebrospinal fluid [%], and hemisphere (left, right).

Please cite this article in press as: S. Casjens, et al., Association of exposure to manganese and iron with striatal and thalamic GABA and other neurometabolites — Neuroimaging results from the WELDOX II study, Neurotoxicology (2017), http://dx.doi.org/10.1016/j.neuro.2017.08.004

4. Discussion

This study employs a non-invasive MRI/MRS technique to quantify the concentrations of GABA and other neurometabolites in the striatum and thalamus of welders exposed to airborne Mn and Fe in an occupational environment, along with several other study groups. Differences in metal exposure were assessed by study group, systemic biomarkers (MnB, SF and SFe), metal accumulation in brain regions of interest (R1, R2*), as well as airborne exposure to Mn and Fe in active welders only. Based on the data acquired, we observed that MRI measures of metal accumulation rather than biomarkers of systemic exposures to metals were associated with the neurometabolite concentrations in the VOIs under study. Airborne exposure was not associated with neurometabolite concentrations.

An advantage of this neuroimaging study is its large size facing the efforts to recruit and investigate men on a voluntary basis for MRI/MRS. Notably, neuroimaging was conducted with a median time lag of six weeks regarding the shift measurements in active welders. This and the relatively low airborne exposure among active welders with median respirable Mn of 23 $\mu g/m^3$, which is in the range of the German OEL of 20 $\mu g/m^3$, may explain the rather similar GABA concentrations among the different study groups. By contrast to a report of increased GABA in a small group of Chinese smelters in a thalamus/basal ganglia VOI (Dydak et al., 2011), we did not find any statistically significant differences between welders and other study groups. Methodological challenges arise due to the low GABA concentration and overlapping spectra (Aufhaus et al., 2013; Mullins et al., 2014) resulting in a larger variability and lower sensitivity to measure GABA. Furthermore, the manual placing of VOIs and ROIs is subject to the expertise of the observer, which we controlled by independent raters.

The neurometabolite concentrations within the various VOIs were strongly correlated. This may indicate a VOI-specific metabolome, beyond the macroscopic neuroanatomical structures GM, WM and CSF. This correlation is weaker with GABA, which may be due to the larger variability and lower sensitivity to measure GABA. Glu is a major transmitter for excitatory neurons and precursor of GABA, which is the major inhibitory neurotransmitter in the adult brain (Bak et al., 2006; Beleboni et al., 2004). The Gln/Glu-GABA cycle reflects interactions between astrocytes and neurons, as only astrocytes synthesize Gln (Aschner et al., 1992). Here, we observed significant correlations between GABA, Glu, and Glx in the striatum, but not in the thalamus. Mn accumulation in astrocytes has been associated with the disruption of striatal Gln/Glu-GABA cycle (Bak et al., 2006). This may be reflected in lower concentrations of GABA, Glu, and Gln in specific brain regions, which may explain the observed correlation, although the results from other studies are inconsistent (Sidoryk-Wegrzynowicz and Aschner, 2013).

Also MnB and SF as measures of systemic exposure to Mn and Fe were not associated with GABA and Glx. We further used R1 as exposure metric for brain metal accumulation and found a weak association of R1 in ROIs of the GP with lower levels of both neurometabolites in the striatum and thalamus. This effect remained rather stable in all models, but did not reach statistical significance. Furthermore, R2* in GP influenced Glx in the VOIs in an opposite direction. R2* is commonly used to assess brain iron content (Fitsanakis et al., 2006). Abnormal accumulation of brain iron has been detected in various neurodegenerative diseases (Rouault, 2013), but the contribution of iron overload to the brain metabolism remains unclear.

The energy demand of the brain is especially high, where iron plays a major role (Ward et al., 2014). Creatine is a regulator of energy homeostasis in the brain and influences GABAergic and glutamatergic neurotransmission, among other functions (Joncquel-Chevalier Curt et al., 2015). Its concentration in GM is higher than in WM, reflecting higher ATP metabolism (Hetherington et al., 2001). Lower concentrations of creatine were observed in the basal ganglia (Mak et al., 2009). Creatine had been found stable and was used as internal reference for the voxel content of GABA when estimating Mn or other effects (Chang et al., 2009; Dydak et al., 2011). However, in our data tCr was lower in welders and PD or HC patients than in controls, and we observed a negative association with R1 in GP. Therefore, tCr is likely not a "neutral" neurometabolite to adjust effects of redox-active metals on GABA. Of note, creatine synthesis usually occurs in kidney and liver where the metabolism is subject to influences of ingestion, aging and other factors (Joncquel-Chevalier Curt et al., 2015). This would implicate a wider range of potential covariates when exploring the tCr content of the brain.

As GABA concentrations are highest in GM, precise tissue segmentation is important (Harris et al., 2015). Also microstructural changes, for example of the Fe content and myelination, might influence the GABA determination (Lorio et al., 2014). Besides neurotoxic or neurodegenerative effects of Mn and Fe on GM, also a methodological problem should be considered. Both metals correlate with MRI parameters such as R1 or R2* and can thus influence the GM-WM contrast (Lorio et al., 2014; Zhang et al., 2009).Alternative segmentation procedures should be tested when studying metal effects.

5. Conclusions

Our data does not show an association of any measure of exposure with the MRS-derived GABA concentration. However, the exposure levels of our welders were low. Our results do not provide evidence that striatal or thalamic GABA was different in Mn-exposed workers or patients with PD or HC as compared to controls. However, tCr was lower in these study groups than in controls. We further showed that the content of all neurometabolites in the VOIs was lower with higher R1 indicating an influence of the metal accumulation in brain regions of interest.

Acknowledgements

The WELDOX II study was supported by a grant from the Employer's Liability Insurance Association for Wood and Metals (Berufsgenossenschaft Holz und Metall). UD, SD, DE, and CLY were supported through NIH/NIEHS grant R01ES020529. MA was supported by NIH grant R01010563. The determination of manganese in welding fumes was performed at the Institute for Occupational Safety and Health of the German Social Accident Insurance (IFA), Sankt Augustin, Germany. We thank Dr. Katrin Pitzke and Tobias Schwank for support in presenting these analyses. We appreciate the scientific support of Burkhard Mädler from PHILIPS, Germany.

Appendix A. Supplementary data

Supplementary data associated with this article can be found, in the online version, at http://dx.doi.org/10.1016/j.neuro.2017.08.004.

References

Öz, G., Alger, J.R., Barker, P.B., Bartha, R., Bizzi, A., Boesch, C., et al., 2014. Clinical proton MR spectroscopy in central nervous system disorders. Radiology 270 (3), 658–679.
Aguirre, J.D., Culotta, V.C., 2012. Battles with iron: manganese in oxidative stress protection. J. Biol. Chem. 287 (17), 13541–13548.
Aschner, M., Gannon, M., Kimelberg, H.K., 1992. Manganese uptake and efflux in cultured rat astrocytes. J. Neurochem. 58 (2), 730–735.
Ashburner, J., Friston, K.J., 2005. Unified segmentation. Neuroimage 26 (3), 839–851.

Aufhaus, E., Weber-Fahr, W., Sack, M., Tunc-Skarka, N., Oberthuer, G., Hoerst, M., et al., 2013. Absence of changes in GABA concentrations with age and gender in the human anterior cingulate cortex: a MEGA-PRESS study with symmetric editing pulse frequencies for macromolecule suppression. Magn. Reson. Med. 69 (2), 317–320.

Bak, L.K., Schousboe, A., Waagepetersen, H.S., 2006. The glutamate/GABA-glutamine cycle: aspects of transport, neurotransmitter homeostasis and ammonia transfer. J. Neurochem. 98 (3), 641–653.

Beleboni, R.O., Carolino, R.O.G., Pizzo, A.B., Castellan-Baldan, L., Coutinho-Netto, J., dos Santos, W.F., et al., 2004. Pharmacological and biochemical aspects of GABAergic neurotransmission: pathological and neuropsychobiological relationships. Cell Mol. Neurobiol. 24 (6), 707–728.

Bouchard, M., Mergler, D., Baldwin, M.E., Panisset, M., 2008. Manganese cumulative exposure and symptoms: a follow-up study of alloy workers. Neurotoxicology 29 (4), 577–583.

Bowman, A.B., Aschner, M., 2014. Considerations on manganese (Mn) treatments for in vitro studies. Neurotoxicology 41, 141–142.

Casjens, S., Henry, J., Rihs, H.-P., Lehnert, M., Raulf, M., Welge, P., et al., 2014. Influence of welding fume on systemic iron status. Ann. Occup. Hyg. 58 (9), 1143–1154.

Chang, Y., Woo, S.-T., Lee, J.-J., Song, H.-J., Lee, H.J., Yoo, D.-S., et al., 2009. Neurochemical changes in welders revealed by proton magnetic resonance spectroscopy. Neurotoxicology 30 (6), 950–957.

Chen, P., Chakraborty, S., Mukhopadhyay, S., Lee, E., Paoliello, M.M.B., Bowman, A.B., et al., 2015. Manganese homeostasis in the nervous system. J. Neurochem. 134 (4), 601–610.

Chowdhury, F.A., O'Gorman, R.L., Nashef, L., Elwes, R.D., Edden, R.A., Murdoch, J.B., et al., 2015. Investigation of glutamine and GABA levels in patients with idiopathic generalized epilepsy using MEGAPRESS. J. Magn. Reson. Imaging 41 (3), 694–699.

Dharmadhikari, S., Ma, R., Yeh, C.-L., Stock, A.-K., Snyder, S., Zauber, S.E., et al., 2015. Striatal and thalamic GABA level concentrations play differential roles for the modulation of response selection processes by proprioceptive information. Neuroimage 120, 36–42.

Dydak, U., Jiang, Y.-M., Long, L.-L., Zhu, H., Chen, J., Li, W.-M., et al., 2011. In vivo measurement of brain GABA concentrations by magnetic resonance spectroscopy in smelters occupationally exposed to manganese. Environ. Health Perspect. 119 (2), 219–224.

Dydak, U., Edmondson, D.A., Zauber, S.E., 2016. Magnetic resonance spectroscopy in Parkinsonian disorders. In: Öz, G. (Ed.), Magnetic Resonance Spectroscopy of Degenerative Brain Diseases. Springer International Publishing, Switzerland, pp. 71–102.

Ellingsen, D.G., Chashchin, M., Berlinger, B., Konz, T., Zibarev, E., Aaseth, J., et al., 2014. Biomarkers of iron status and trace elements in welders. J. Trace Elem. Med. Biol. 28 (3), 271–277.

Emir, U.E., Tuite, P.J., Oz, G., 2012. Elevated pontine and putamenal GABA levels in mild-moderate Parkinson disease detected by 7 tesla proton MRS. PLoS One 7 (1), e30918.

Fitsanakis, V.A., Zhang, N., Avison, M.J., Gore, J.C., Aschner, J.L., Aschner, M., 2006. The use of magnetic resonance imaging (MRI) in the study of manganese neurotoxicity. Neurotoxicology 27 (5), 798–806.

Flynn, M.R., Susi, P., 2010. Manganese, iron, and total particulate exposures to welders. J. Occup. Environ. Hyg. 7 (2), 115–126.

Guilarte, T.R., McGlothan, J.L., Degaonkar, M., Chen, M.-K., Barker, P.B., Syversen, T., et al., 2006. Evidence for cortical dysfunction and widespread manganese accumulation in the nonhuman primate brain following chronic manganese exposure: a 1H-MRS and MRI study. Toxicol. Sci. 94 (2), 351–358.

Guilarte, T.R., 2013. Manganese neurotoxicity: new perspectives from behavioral, neuroimaging, and neuropathological studies in humans and non-human primates. Front Aging Neurosci. 5, 23.

Gwiazda, R., Lucchini, R., Smith, D., 2007. Adequacy and consistency of animal studies to evaluate the neurotoxicity of chronic low-level manganese exposure in humans. J. Toxicol. Environ. Health A 70 (7), 594–605.

Harris, A.D., Puts, N.A.J., Edden, R.A.E., 2015. Tissue correction for GABA-edited MRS: considerations of voxel composition, tissue segmentation, and tissue relaxations. J. Magn. Reson. Imaging 42 (5), 1431–1440.

Hebisch, R., Fricke, H.H., Hahn, J.U., Lahaniatis, M., Maschmeier, C.P., Mattenklott, M., 2005. Sampling and determining aerosols and their chemical compounds, in: The MAK collection for occupational health and safety, Part III. Air Monit. Methods 3–40.

Hetherington, H.P., Spencer, D.D., Vaughan, J.T., 2001. Pan JW: Quantitative ^{31}P spectroscopic imaging of human brain at 4 Tesla: assessment of gray and white matter differences of phosphocreatine and ATP. Magn. Reson. Med. 45 (1), 46–52.

Iannilli, E., Gasparotti, R., Hummel, T., Zoni, S., Benedetti, C., Fedrighi, C., et al., 2016. Effects of manganese exposure on olfactory functions in teenagers: a pilot study. PLoS One 11 (1), e0144783.

Jiang, H., Wang, J., Rogers, J., Xie, J., 2016. Brain iron metabolism dysfunction in Parkinson's disease. Mol. Neurobiol. 1–24.

Joncquel-Chevalier Curt, M., Voicu, P.-M., Fontaine, M., Dessein, A.-F., Porchet, N., Mention-Mulliez, K., et al., 2015. Creatine biosynthesis and transport in health and disease. Biochimie 119, 146–165.

Kim, J., Wessling-Resnick, M., 2014. Iron and mechanisms of emotional behavior. J. Nutr. Biochem. 25 (11), 1101–1107.

Kim, E.A., Cheong, H.-K., Choi, D.S., Sakong, J., Ryoo, J.W., Park, I., et al., 2007. Effect of occupational manganese exposure on the central nervous system of welders: ^{1}H magnetic resonance spectroscopy and MRI findings. Neurotoxicology 28 (2), 276–283.

Lee, E.-Y., Flynn, M.R., Du, G., Lewis, M.M., Fry, R., Herring, A.H., et al., 2015. T1 relaxation rate (R1) indicates non-linear Mn accumulation in brain tissue of welders with low-level exposure. Toxicol. Sci..

Lee, E.-Y., Flynn, M.R., Du, G., Li, Y., Lewis, M.M., Herring, A.H., et al., 2016. Increased R2* in the caudate nucleus of asymptomatic welders. Toxicol. Sci. 150 (2), 369–377.

Lehnert, M., Pesch, B., Lotz, A., Pelzer, J., Kendzia, B., Gawrych, K., et al., 2012. Exposure to inhalable, respirable, and ultrafine particles in welding fume. Ann. Occup. Hyg. 56 (5), 557–567.

Long, Z., Li, X.-R., Xu, J., Edden, R.A.E., Qin, W.-P., Long, L.-L., et al., 2014. Thalamic GABA predicts fine motor performance in manganese-exposed smelter workers. PLoS One 9 (2), e88220.

Long, Z., Jiang, Y.-M., Li, X.-R., Fadel, W., Xu, J., Yeh, C.-L., et al., 2014a. Vulnerability of welders to manganese exposure – a neuroimaging study. Neurotoxicology 45, 285–292.

Lorio, S., Lutti, A., Kherif, F., Ruef, A., Dukart, J., Chowdhury, R., et al., 2014. Disentangling in vivo the effects of iron content and atrophy on the ageing human brain. Neuroimage 103, 280–289.

Mak, C.S.W., Waldvogel, H.J., Dodd, J.R., Gilbert, R.T., Lowe, M.T.J., Birch, N.P., et al., 2009. Immunohistochemical localisation of the creatine transporter in the rat brain. Neuroscience 163 (2), 571–585.

Mergler, D., Baldwin, M., Belanger, S., Larribe, F., Beuter, A., Bowler, R., et al., 1999. Manganese neurotoxicity, a continuum of dysfunction: results from a community based study. Neurotoxicology 20 (2–3), 327–342.

Mullins, P.G., McGonigle, D.J., O'Gorman, R.L., Puts Nicolaas, A.J., Vidyasagar, R., Evans, C.J., et al., 2014. Current practice in the use of MEGA-PRESS spectroscopy for the detection of GABA. Neuroimage 86, 43–52.

Myers, J.E., teWaterNaude, J., Fourie, M., Zogoe, H.B.A., Naik, I., Theodorou, P., et al., 2003. Nervous system effects of occupational manganese exposure on South African manganese mineworkers. Neurotoxicology 24 (4–5), 649–656.

Pesch, B., Weiss, T., Kendzia, B., Henry, J., Lehnert, M., Lotz, A., et al., 2012. Levels and predictors of airborne and internal exposure to manganese and iron among welders. J. Expo. Sci. Environ. Epidemiol. 22 (3), 291–298.

Provencher, S.W., 1993. Estimation of metabolite concentrations from localized in vivo proton NMR spectra. Magn. Reson. Med. 30 (6), 672–679.

Racette, B.A., Searles Nielsen, S., Criswell, S.R., Sheppard, L., Seixas, N., Warden, M.N., et al., 2017. Dose-dependent progression of parkinsonism in manganese-exposed welders. Neurology 88 (4), 344–351.

Rouault, T.A., 2013. Iron metabolism in the CNS: Implications for neurodegenerative diseases. Nat. Rev. Neurosci. 14 (8), 551–564.

Sabati, M., Maudsley, A.A., 2013. Fast and high-resolution quantitative mapping of tissue water content with full brain coverage for clinically-driven studies. Magn. Reson. Imaging 31 (10), 1752–1759.

Sidoryk-Wegrzynowicz, M., Aschner, M., 2013. Manganese toxicity in the central nervous system: the glutamine/glutamate-gamma-aminobutyric acid cycle. J. Intern. Med. 273 (5), 466–477.

Ward, R.J., Zucca, F.A., Duyn, J.H., Crichton, R.R., Zecca, L., 2014. The role of iron in brain ageing and neurodegenerative disorders. Lancet Neurol. 13 (10), 1045–1060.

Zhang, N., Fitsanakis, V.A., Erikson, K.M., Aschner, M., Avison, M.J., Gore, J.C., 2009. A model for the analysis of competitive relaxation effects of manganese and iron in vivo. NMR Biomed. 22 (4), 391–404.

Zheng, W., Fu, S.X., Dydak, U., Cowan, D.M., 2011. Biomarkers of manganese intoxication. Neurotoxicology 32 (1), 1–8.

Zoni, S., Lucchini, R.G., 2013. Manganese exposure: cognitive, motor and behavioral effects on children: a review of recent findings. Curr. Opin. Pediatr. 25 (2), 255–260.

Zucca, F.A., Segura-Aguilar, J., Ferrari, E., Muñoz, P., Paris, I., Sulzer, D., et al., 2015. Interactions of iron, dopamine and neuromelanin pathways in brain aging and Parkinson's disease. Prog. Neurobiol..

Please cite this article in press as: S. Casjens, et al., Association of exposure to manganese and iron with striatal and thalamic GABA and other neurometabolites — Neuroimaging results from the WELDOX II study, Neurotoxicology (2017), http://dx.doi.org/10.1016/j.neuro.2017.08.004